Teleconnections and interannual variability of the atmosphere

Franco Molteni

European Centre for Medium-Range Weather Forecasts

Outline

- Teleconnection patterns:
  - Definition from observational datasets
  - Dynamical origin and interpretation: review of seminal papers

- Understanding teleconnections from the Indo-Pacific region:
  - Relationship between SST and rainfall variability
  - Comparison between observed and modelled teleconnection in seasonal forecast ensembles: examples from the ECMWF System-4 re-forecasts
  - Differences between diagnostics derived from covariances with SST and rainfall anomalies

Teleconnections: definitions and examples

Teleconnection:

Relationship between anomalies of opposite sign (and/or different variables) in different regions of the world

Teleconnection pattern:

Regional or planetary scale pattern of correlated anomalies

Teleconnections may be induced either by internal atmospheric dynamics or by coupling with other components of the climate system (mainly the tropical oceans)

Teleconnections: definitions and examples

The Southern Oscillation (and its links to El Niño)

Walker and Bliss (1932); Bjerknes (1969)

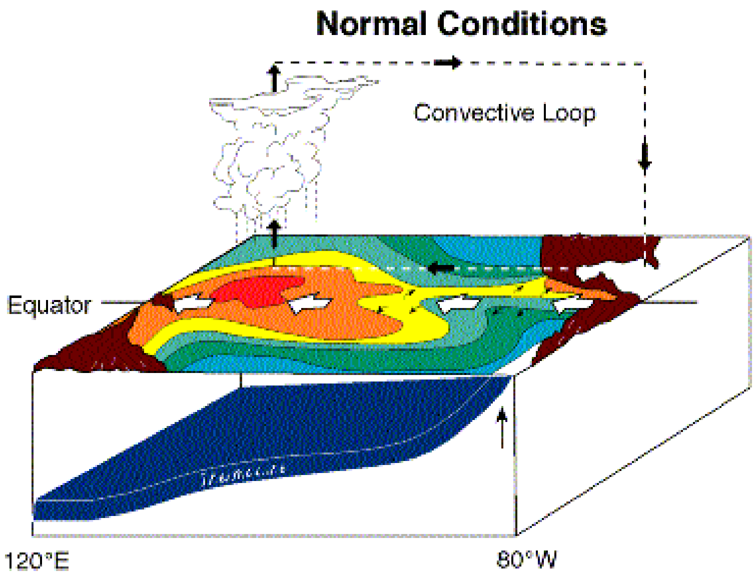

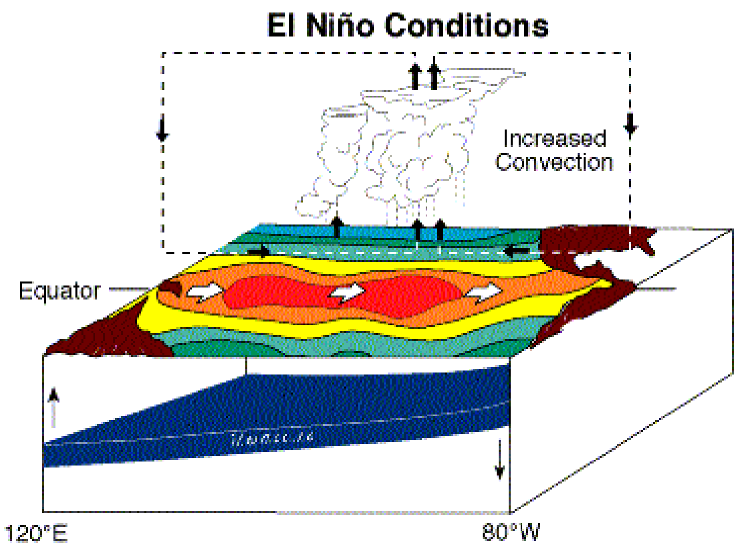

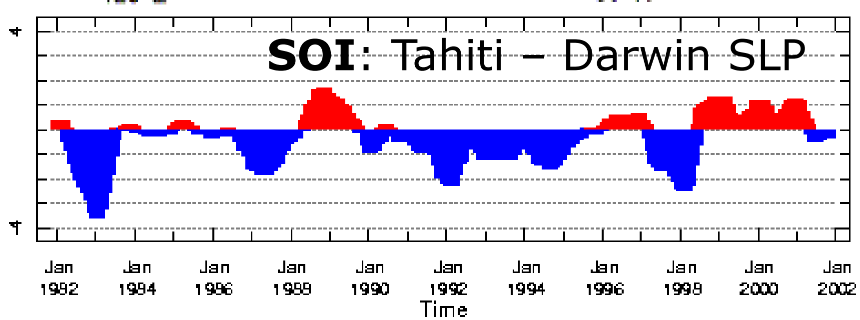

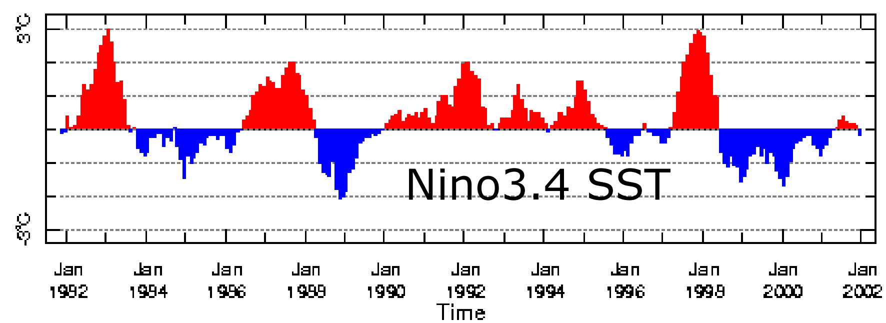

Teleconnections: definitions and examples

The North Atlantic Oscillation

Walker and Bliss (1932)

Van Loon and Rogers (1978)

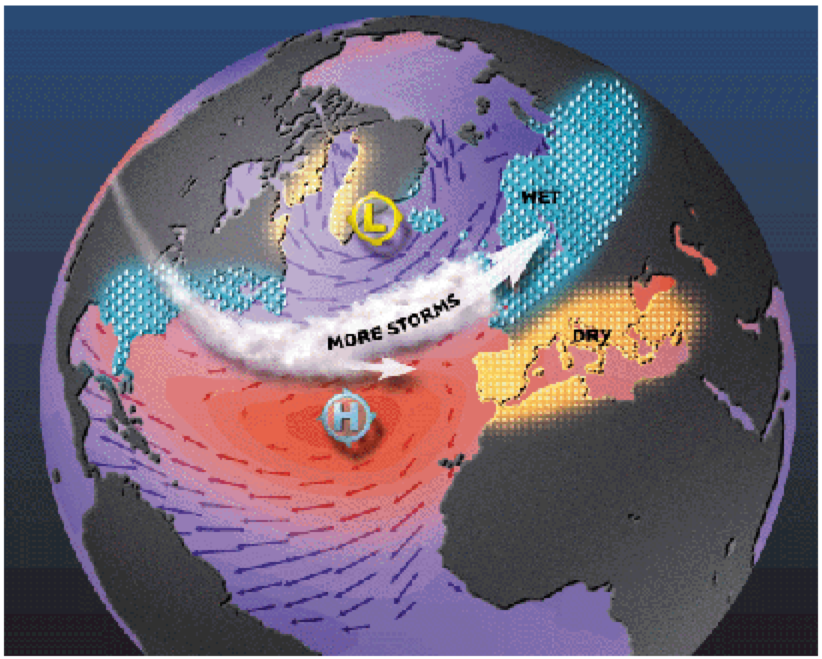

Positive NAO phase

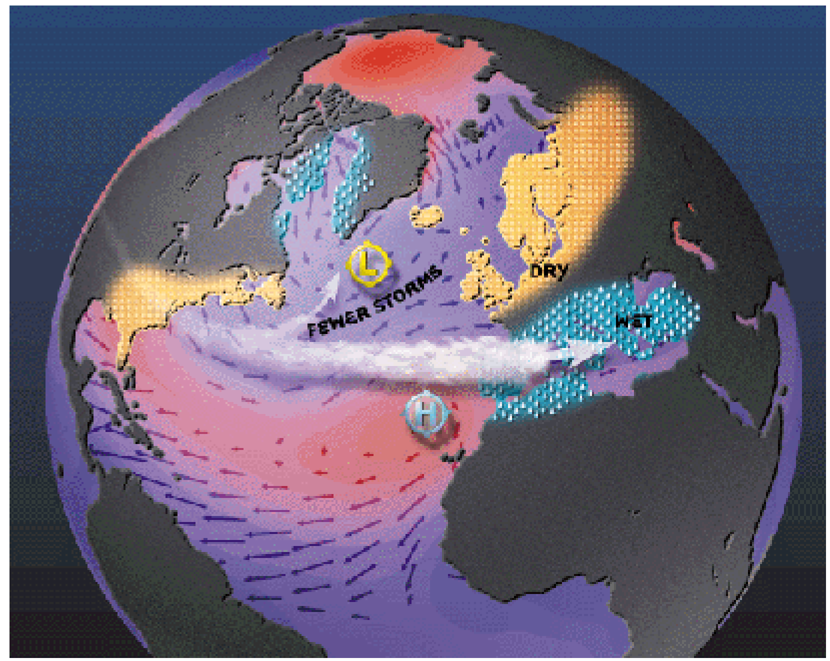

Negative NAO phase

Seminal papers: Wallace and Gutzler 1981

The Pacific / North American (PNA) pattern: correlations

APRIL 1981 JOHN M. WALLACE AND DAVID S. GUTZLER 799

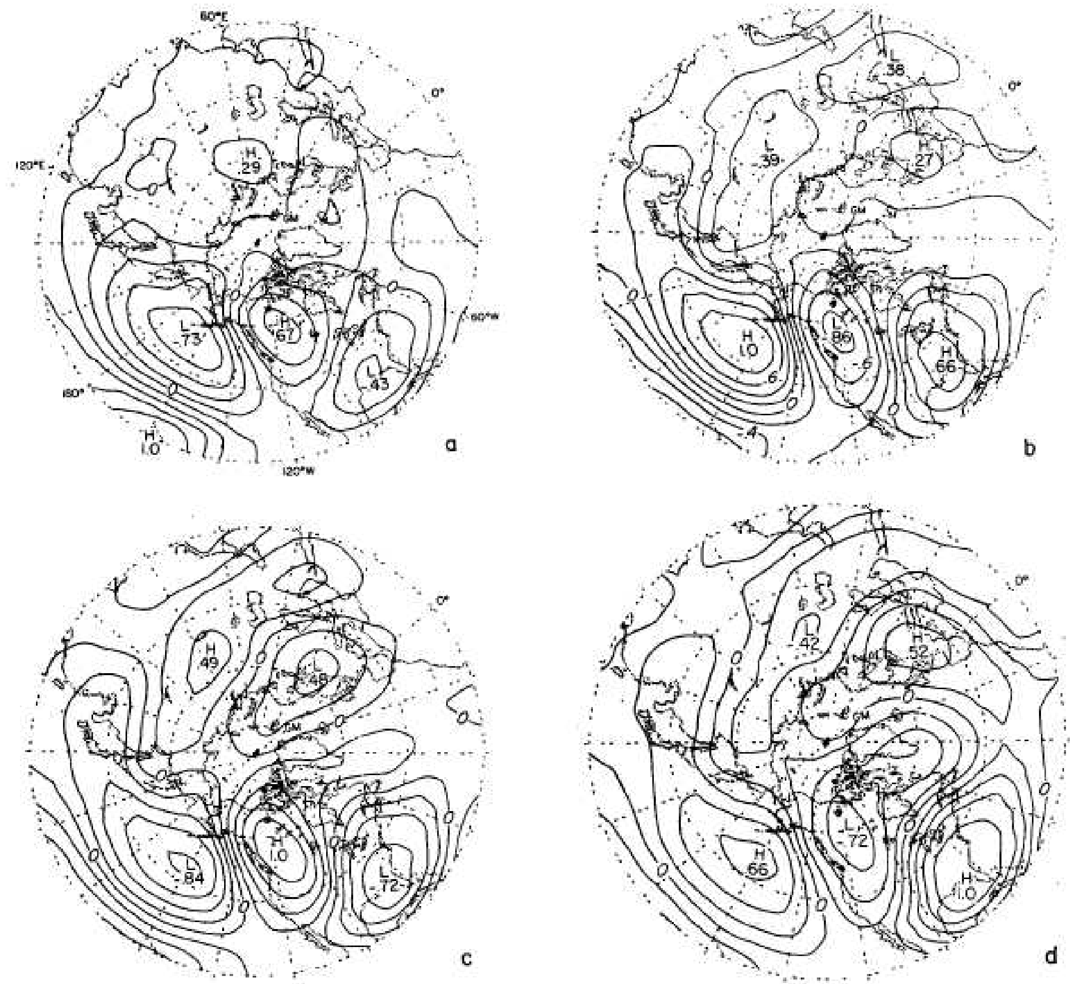

FIG. 16. As in Fig. 12, but for base grid points (a) 20°N, 160°W; (b) 45°N, 165°W; (c) 55°N, 115°W; (d) 30°N, 85°W.

Seminal papers: Wallace and Gutzler 1981

The Pacific / North American (PNA) pattern: composites

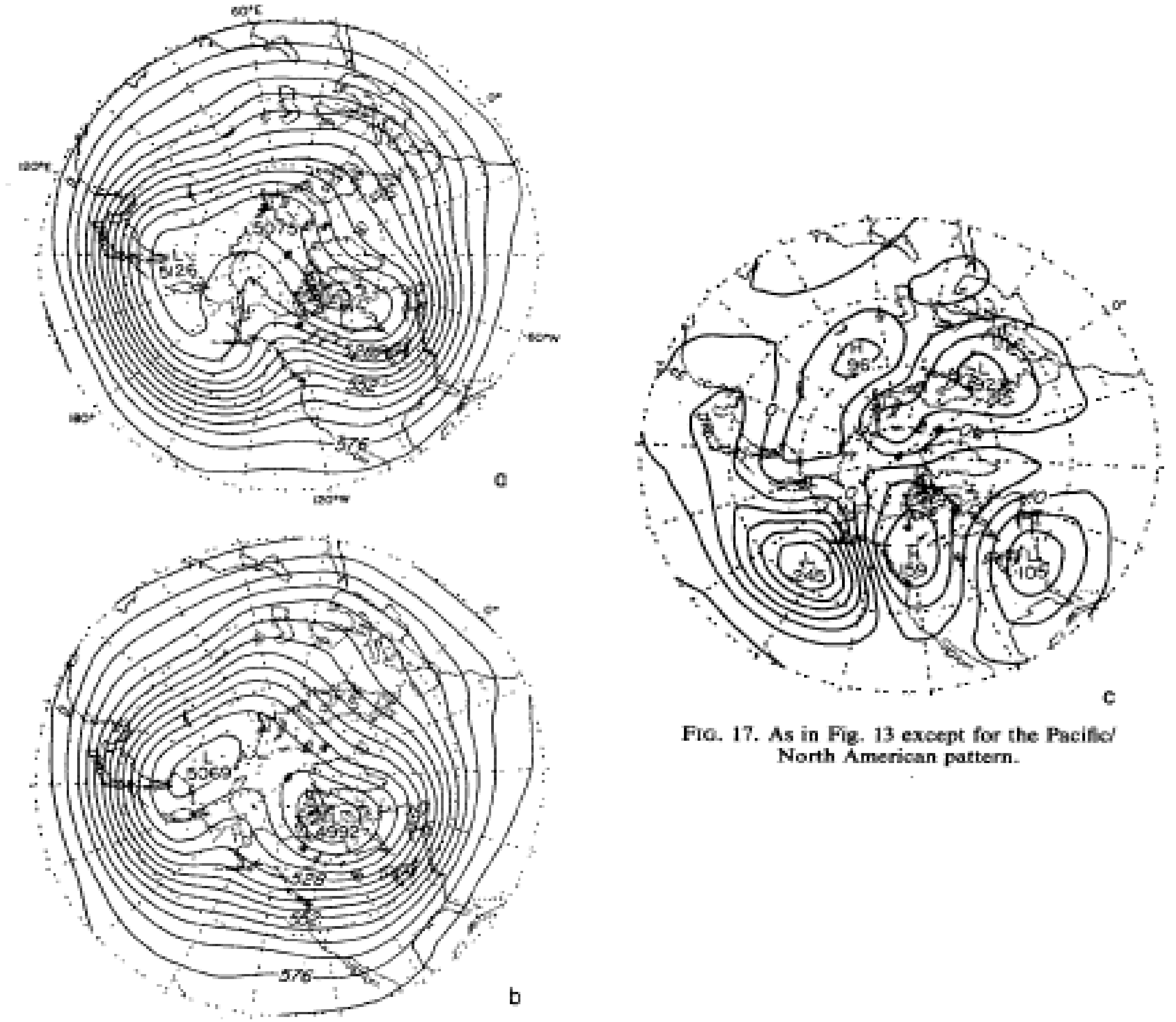

FIG. 17. As in Fig. 13 except for the Pacific/ North American pattern.

Seminal papers: Wallace and Gutzler 1981

Eastern Atlantic (EA) pattern: composites

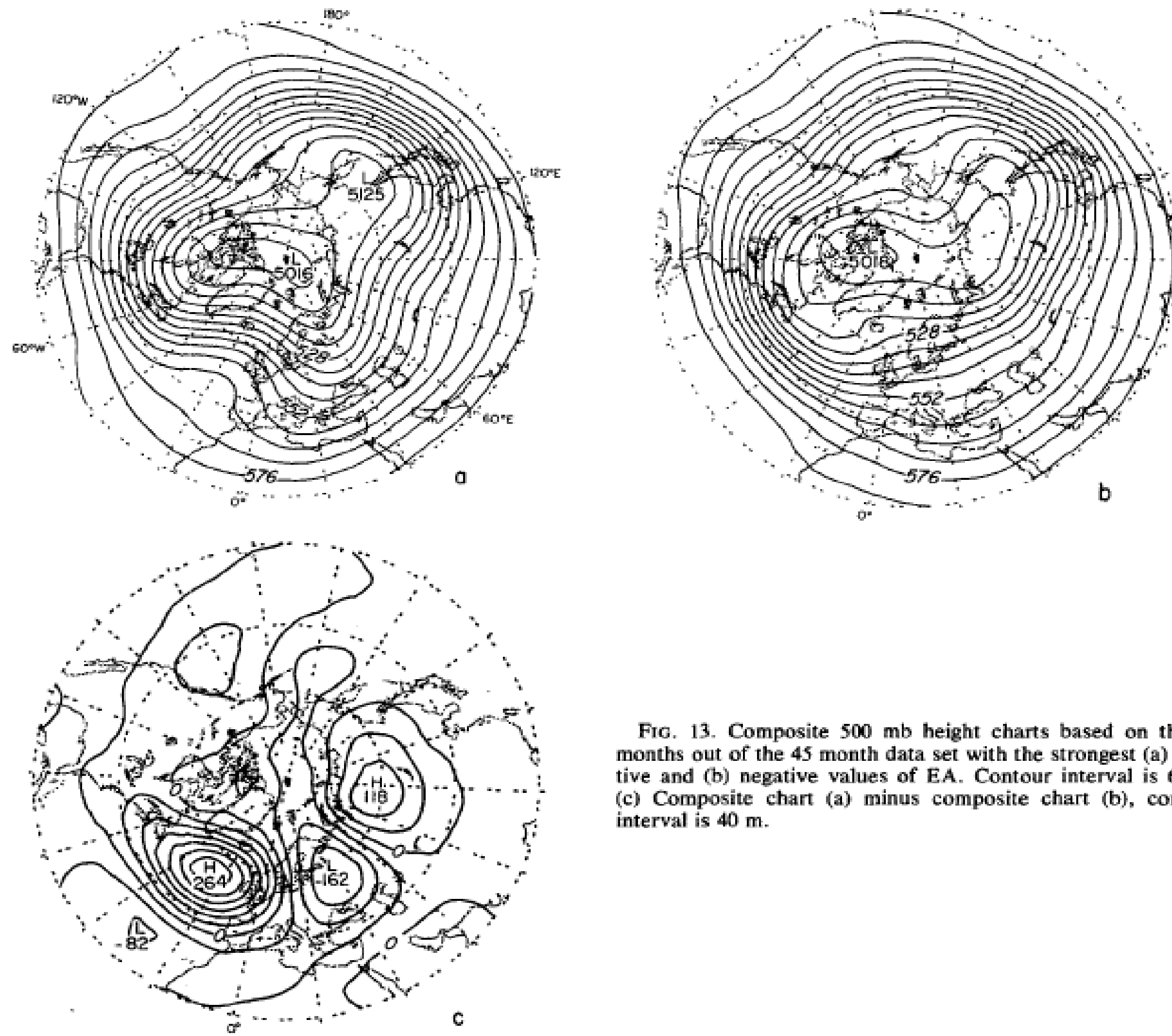

FIG. 13. Composite 500 mb height charts based on the 10 months out of the 45 month data set with the strongest (a) positive and (b) negative values of EA. Contour interval is 60 m. (c) Composite chart (a) minus composite chart (b), contour interval is 40 m.

Seminal papers: Horel and Wallace 1981

a

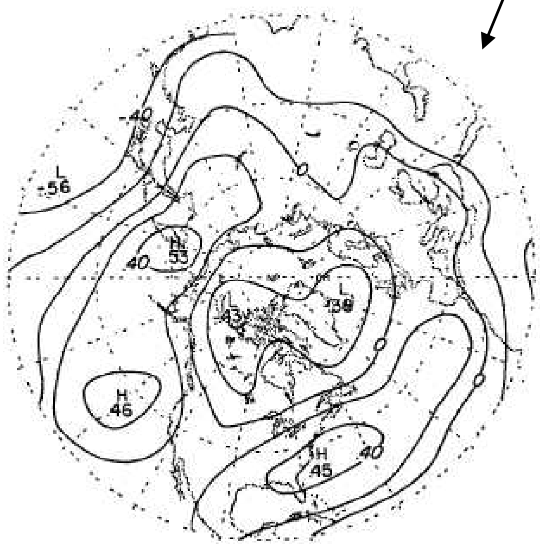

c

Correlation of 700hPa height with
a) PC1 of Eq. Pacific SST
c) SOI index

Schematic diagram of tropical-extratropical teleconnections during El Niño

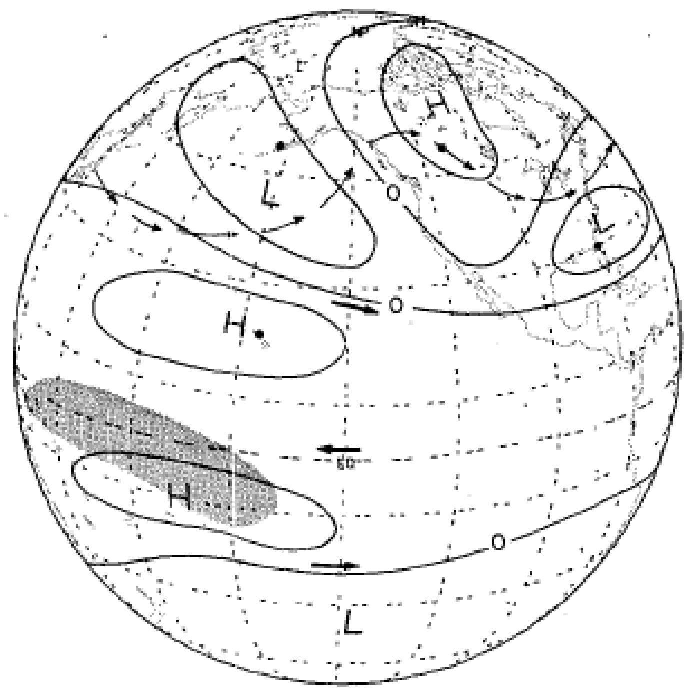

Seminal papers: Gill 1980

Atmospheric response to near-equatorial heating

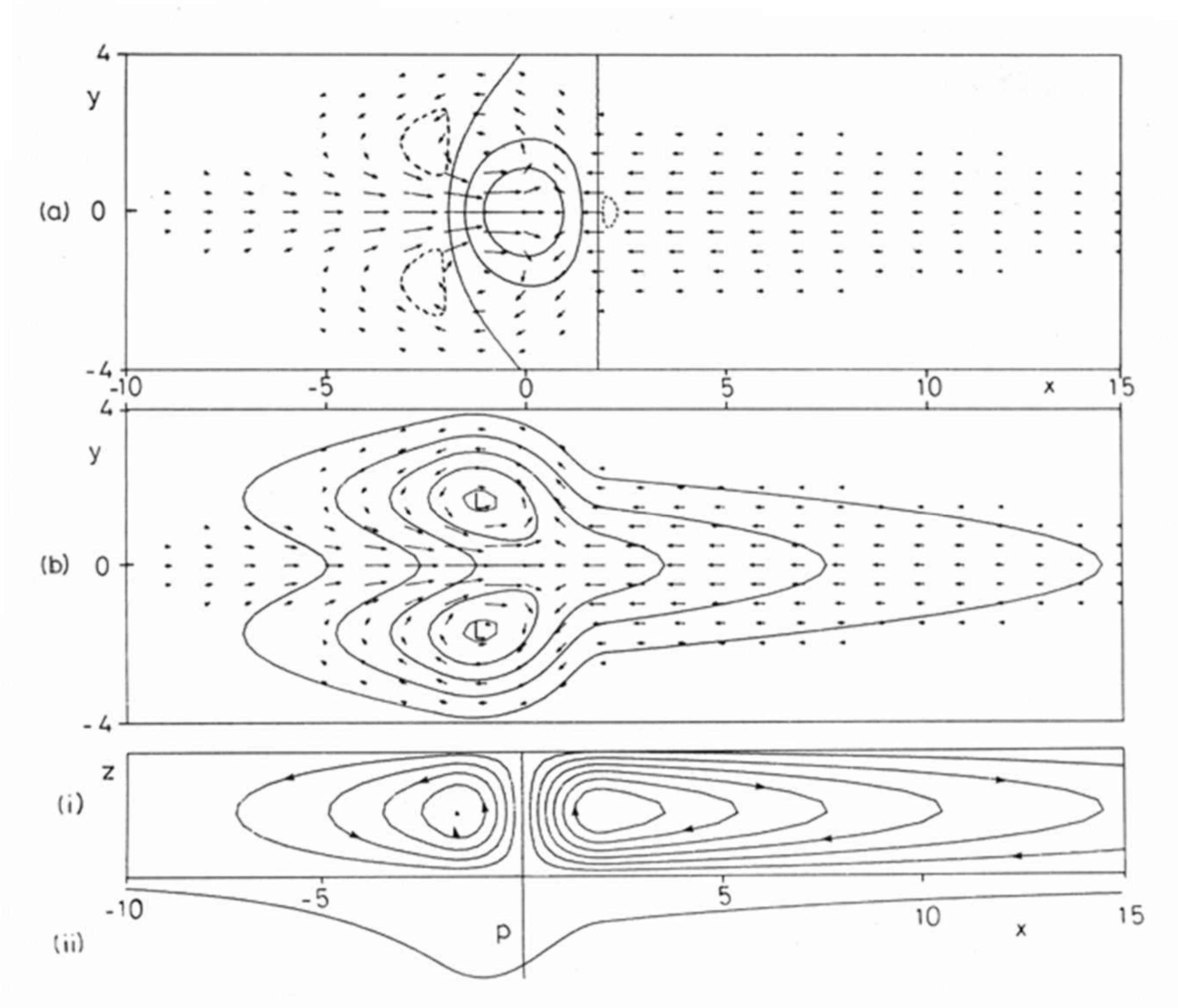

a) Near-surface wind and vertical motion

b) Near-surface wind and sea-level pressure

c) Motion in x-z plane along the Equator

Seminal papers: Hoskins and Karoly 1981

Response to a tropical heat source (15N):

a) height (lon, z) at 18N
b) 300hPa vorticity
c) 300hPa height

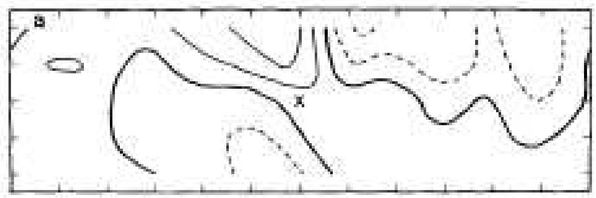

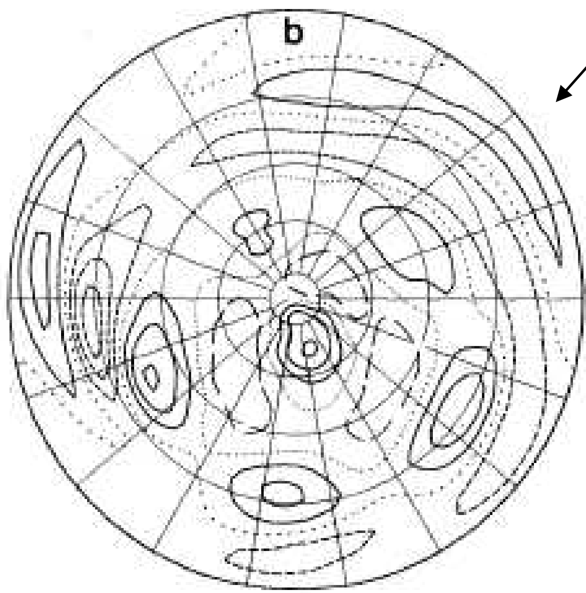

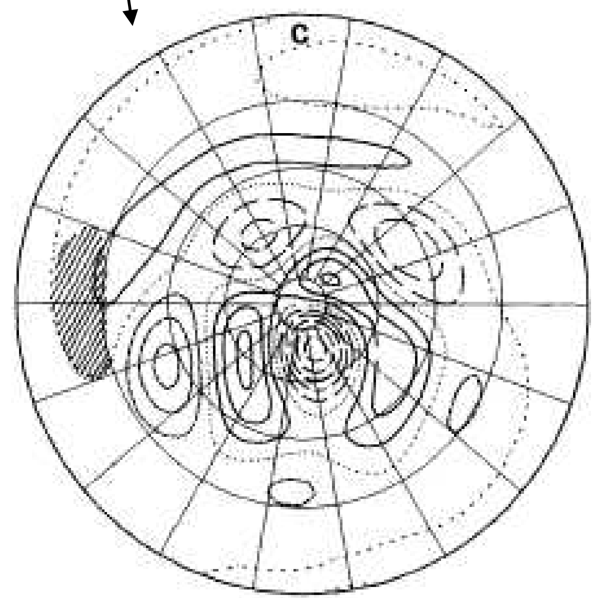

Seminal papers: Simmons Wallace Branstator 1983

First barotropic normal mode at four times during a half-cycle:

East. Atlantic phase
PNA phase

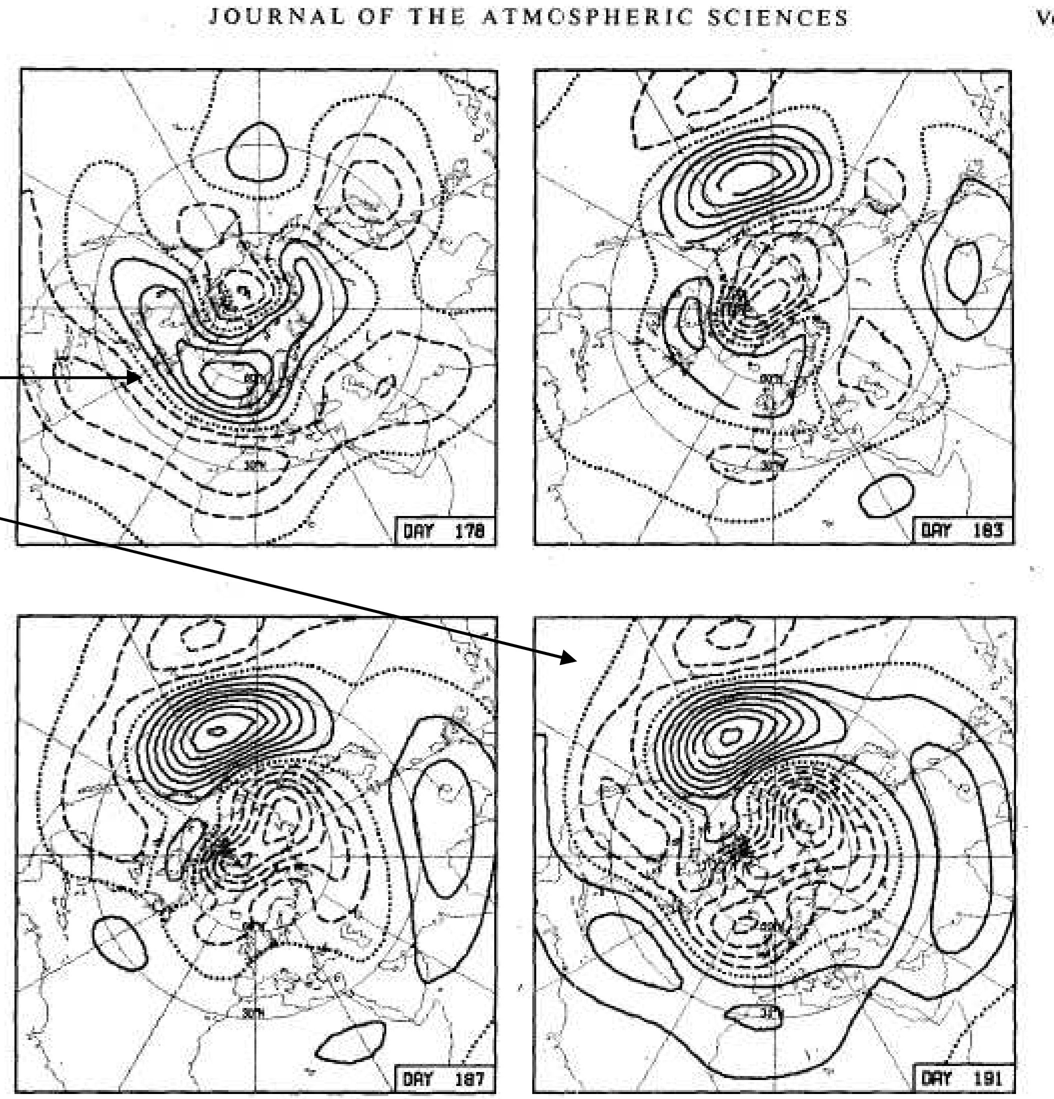

Seminal papers: Sardeshmukh and Hoskins 1988

Definition of Rossby wave source generated by near-equatorial heating

specification of the Rossby wave source S. If we are interested in the generation of Rossby waves, we are interested in the equation

$$\left(\frac{\partial}{\partial t} + \mathbf{v}_\psi \cdot \nabla\right)\zeta = S + F. \qquad (2)$$

Here $\mathbf{v}_\psi$ is the rotational wind associated with ζ. Comparing with (1) we see that we should write the total wind $\mathbf{v}$ in terms of its rotational and divergent components

$$\mathbf{v} = \mathbf{v}_\psi + \mathbf{v}_\chi$$

where $\nabla \cdot \mathbf{v}_\chi = D$. Then (1) may be written in the form of (2) but with

$$S = -\mathbf{v}_\chi \cdot \nabla\zeta - \zeta D. \qquad (3)$$

Seminal papers: Sardeshmukh and Hoskins 1988

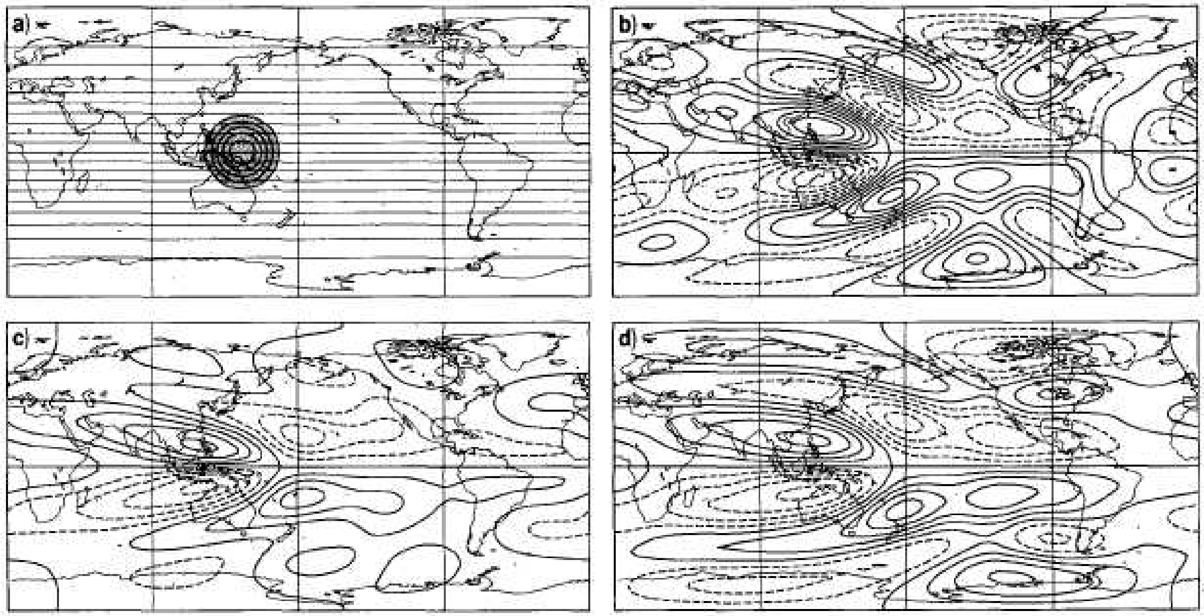

FIG. 1. (a) Basic flow streamfunction (contour interval 10^7 m^2 s^{-1}) and divergence perturbation (shaded; contour interval 10^{-6} s^{-1}). The streamfunction perturbation patterns on day 48 predicted by the linear, partially nonlinear, and fully nonlinear models described in the text are shown in (b), (c) and (d), respectively. The contour interval is 5×10^6 m^2 s^{-1} in all the three panels, and negative values are indicated by dashed contours.

Response to heating in trop. West Pacific

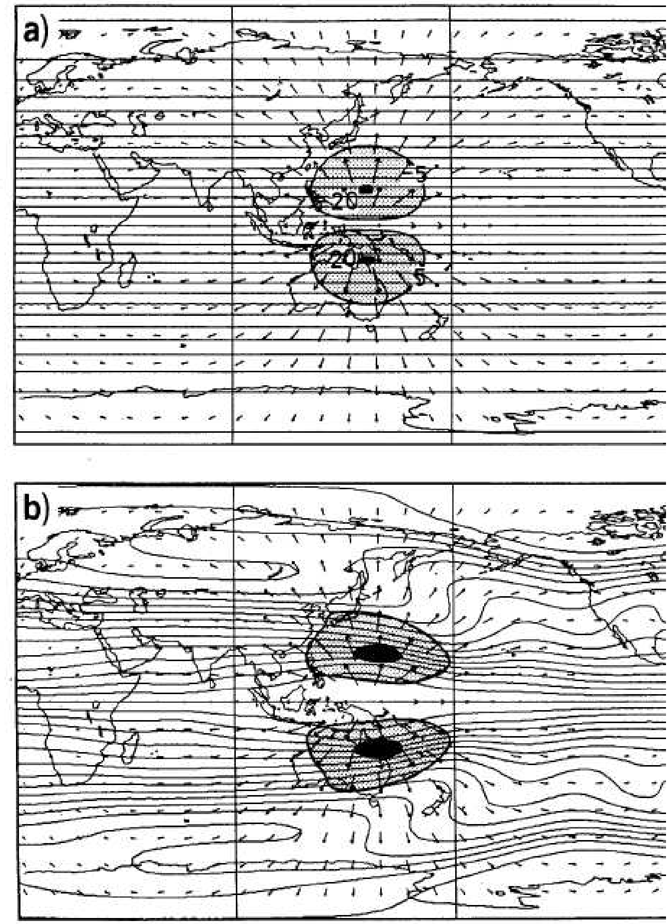

FIG. 2. (a) Rossby wave source S (shaded; units 10^{-11} s^{-2}) on day 0. The steady divergent wind vect
(10^{-5} s^{-1}) that determine this source are also shown. (b) as in (a) but on day 48 of the fully nonlinea
winds in the subtropics are about 5 m s^{-1}.

Rossby wave source
and abs. vorticity

The new ECMWF Seasonal fc. system (Sys-4)

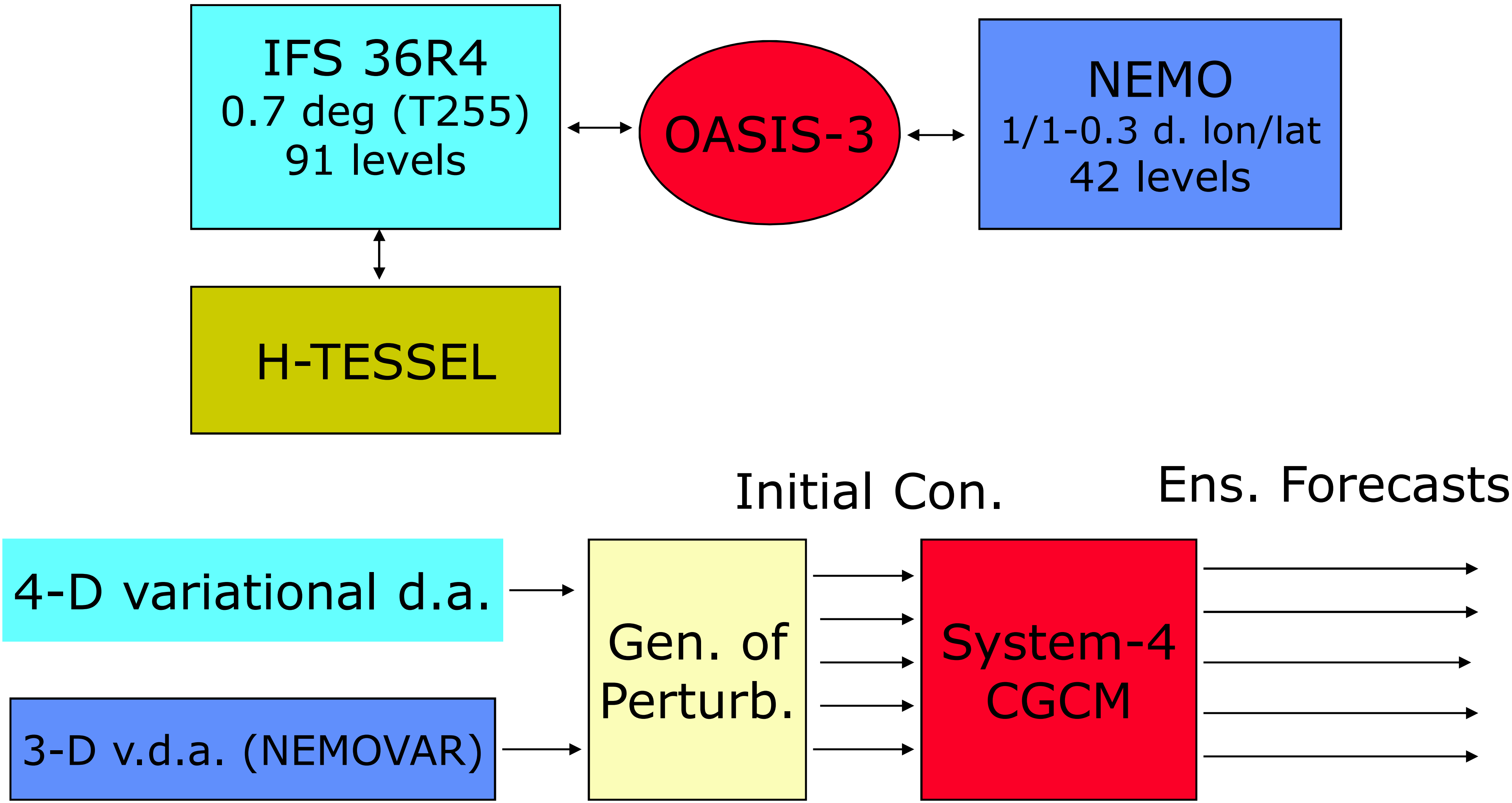

ECMWF System 4: main features

- **Operational forecasts**
  - 51-member ensemble from 1st day of the month
  - released on the 8th
  - 7-month integration

- **Experimental ENSO outlook**
  - 13-month extension from 1st Feb/May/Aug/Nov
  - 15-member ensemble

- **Re-forecast set**
  - 30 years, start dates from 1 Jan 1981 to 1 Dec 2010
  - 15-member ensembles, 7-month integrations
  - 13-month extension from 1st Feb/May/Aug/Nov

Predictability of teleconnections in Sys4: Nino3.4, IOD SST

Nino3.4
DJF

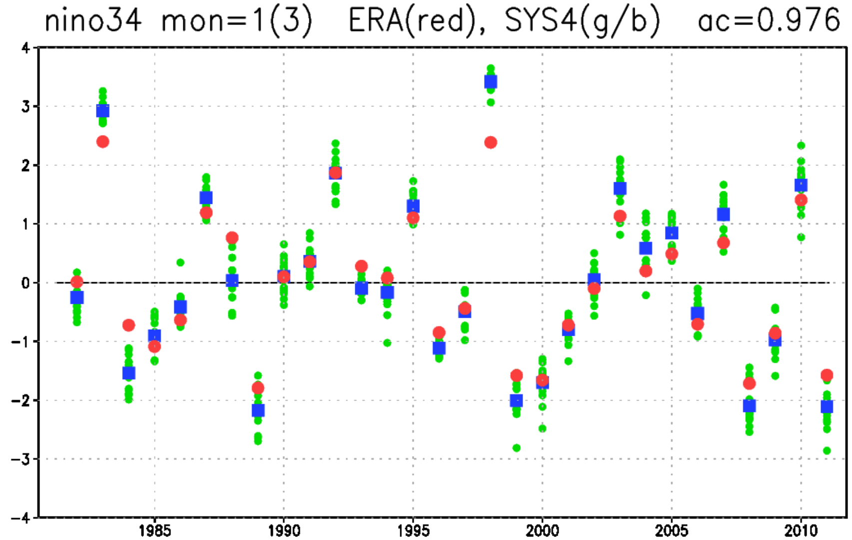

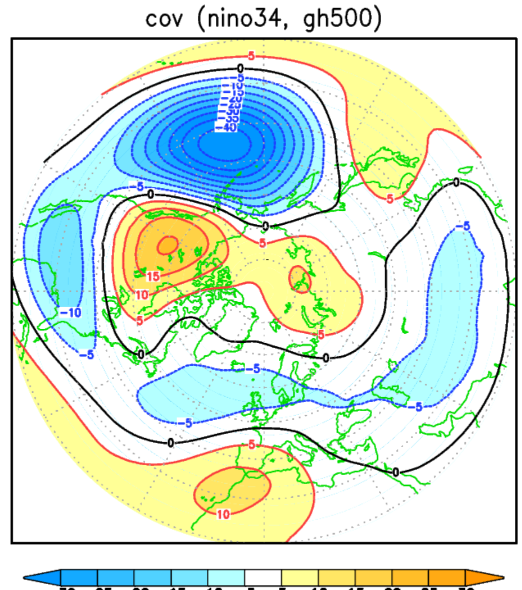

IOD
SON

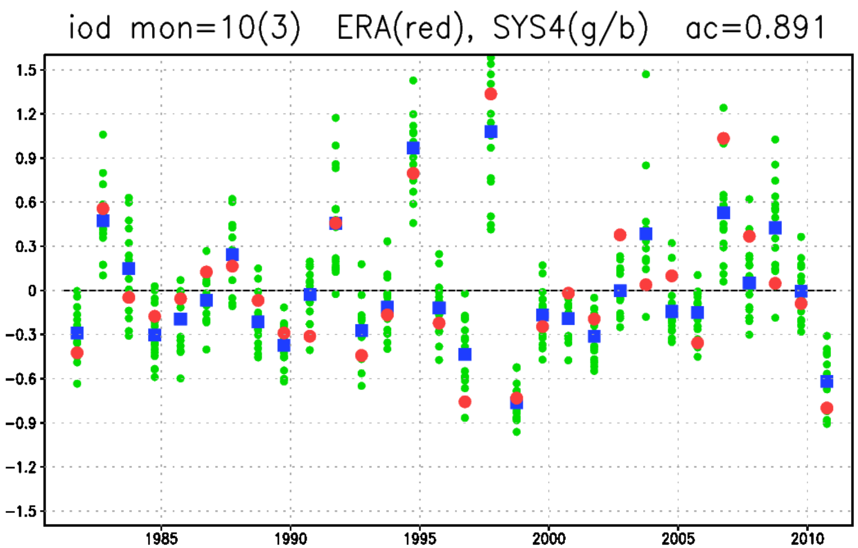

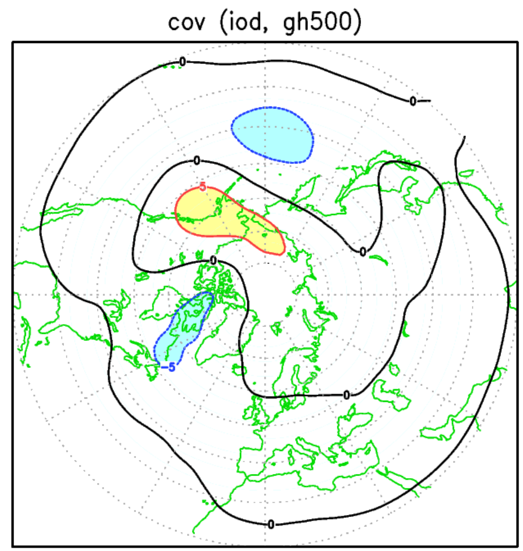

Local correlation SST – precip, DJF

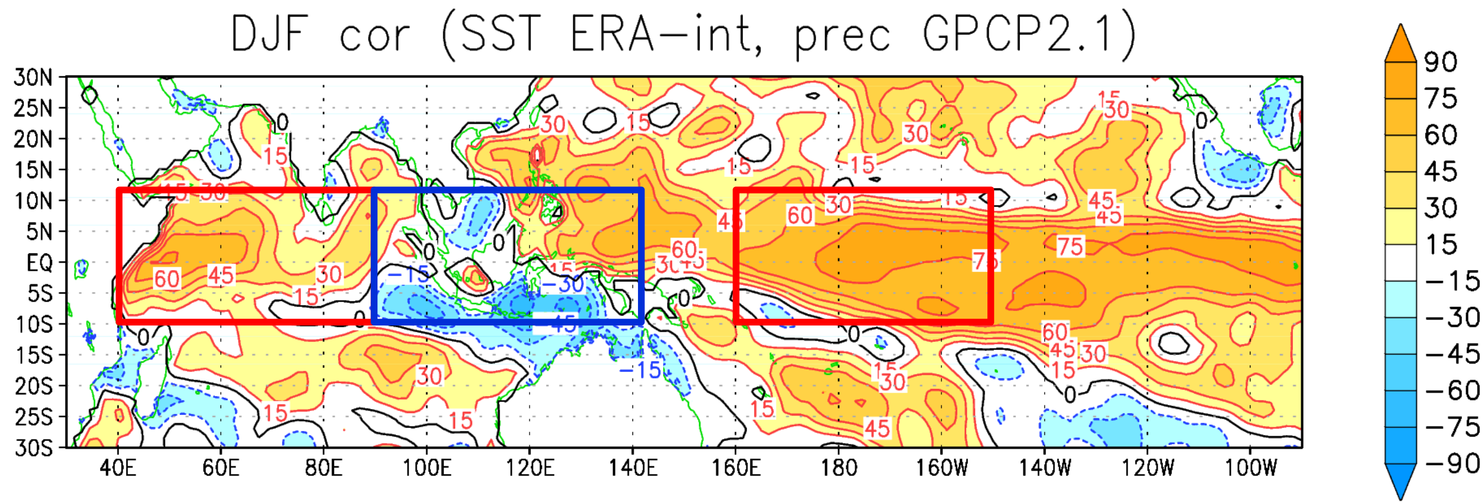

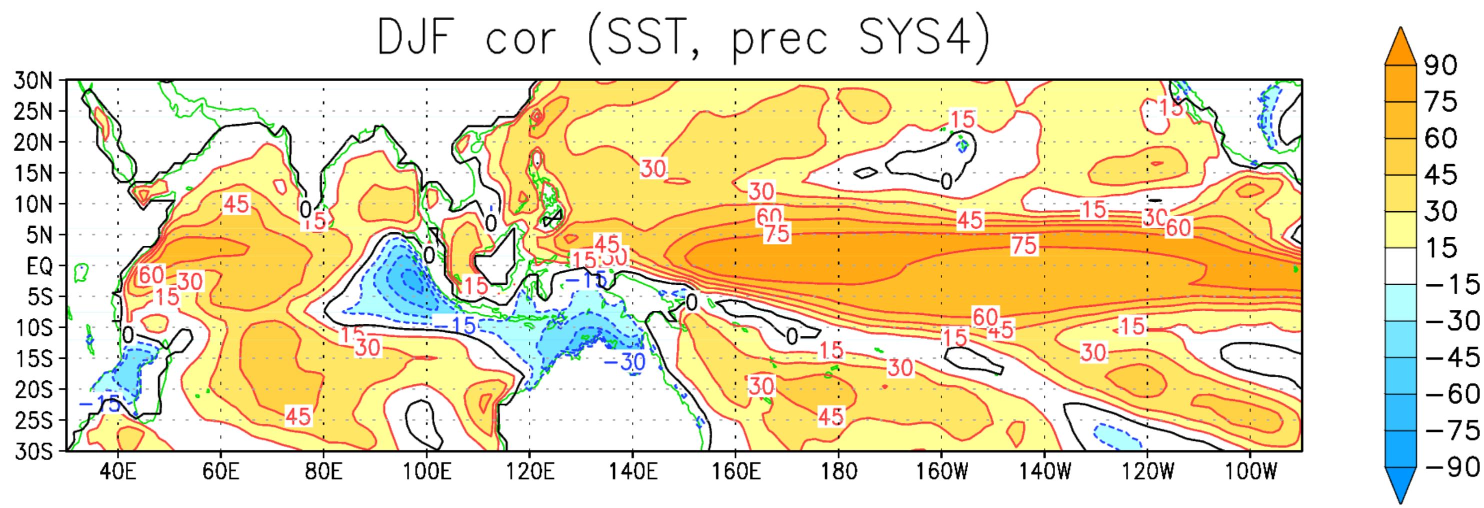

SST teleconnections in DJF: ERA Interim

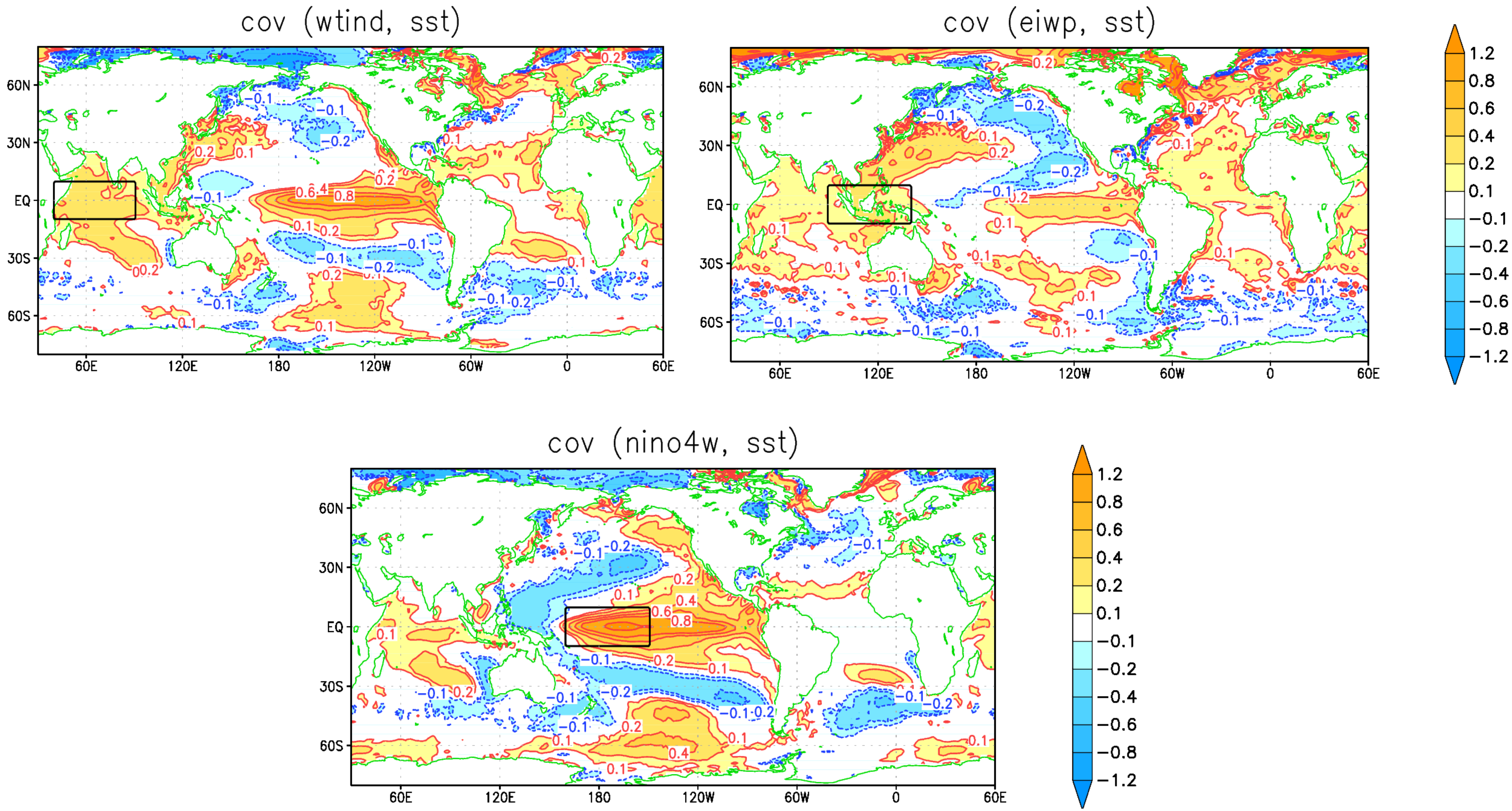

SST teleconnections in DJF: System 4 (from Nov.)

cov (wtind, sst)

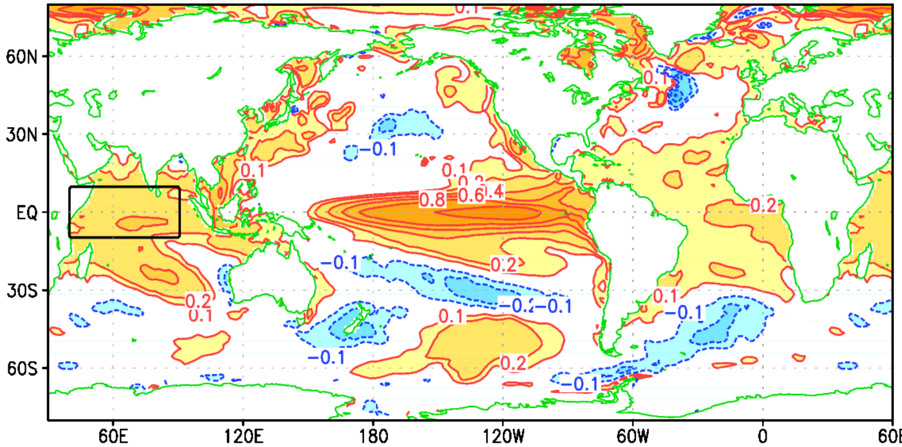

cov (eiwp, sst)

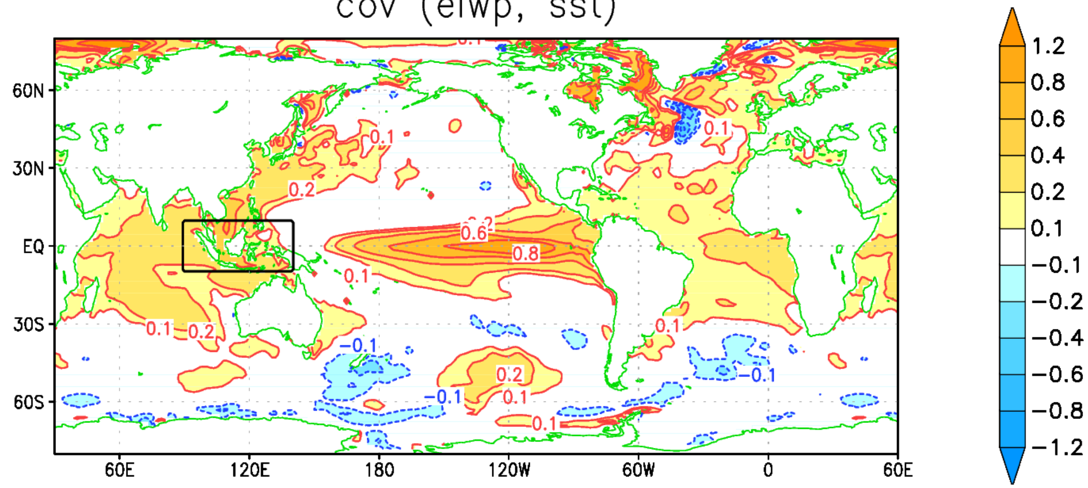

cov (nino4w, sst)

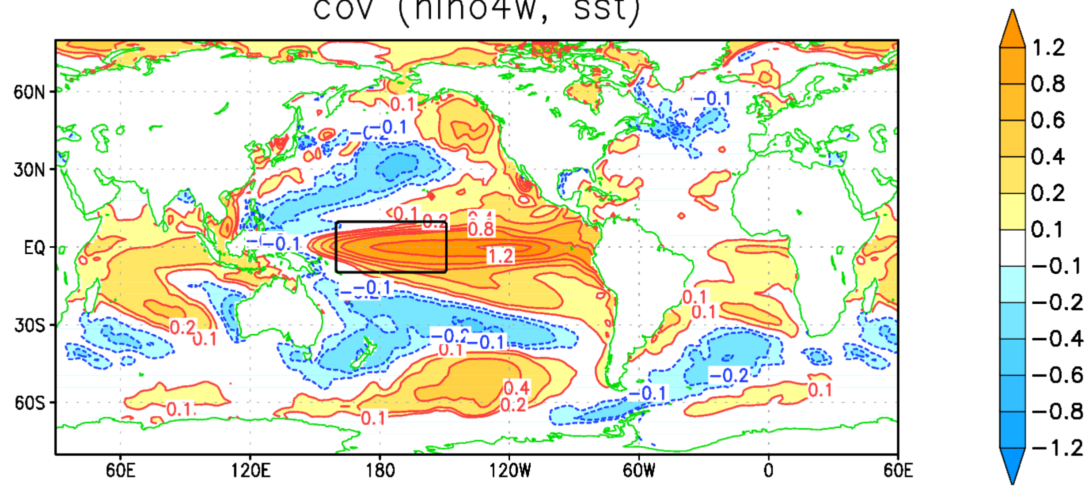

Precip. teleconnections in DJF: GPCP 2.2

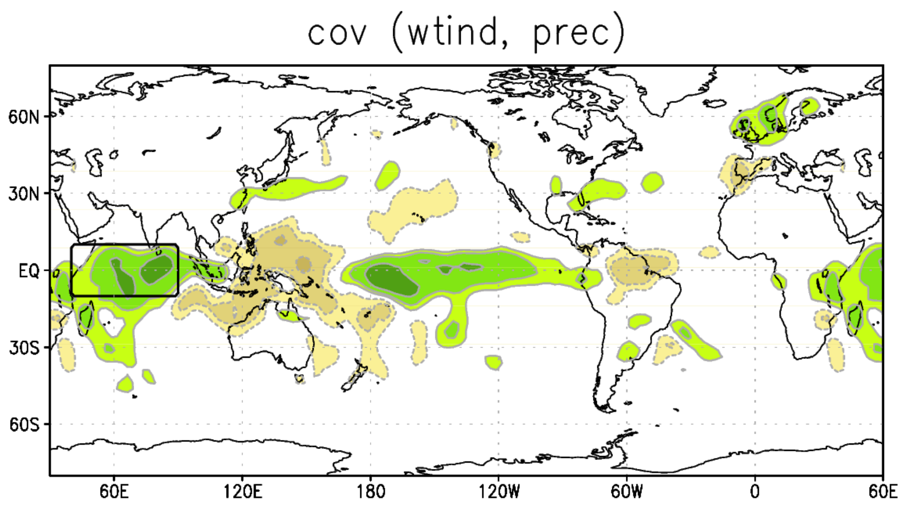

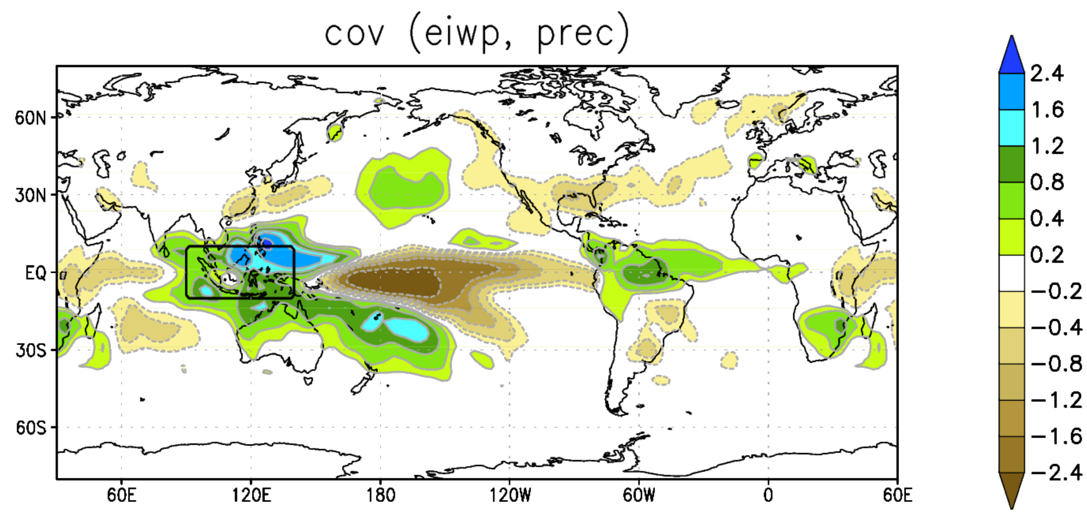

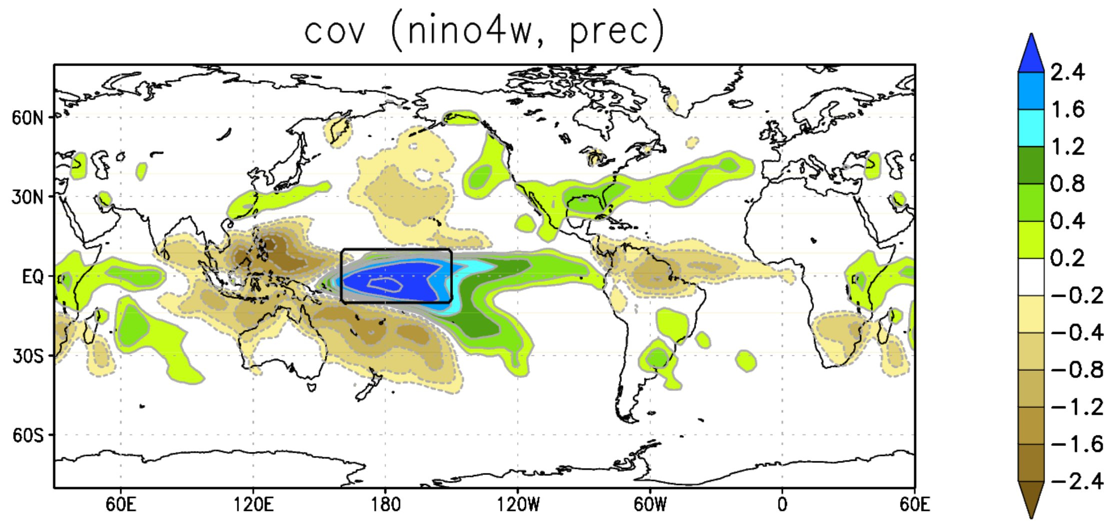

Precip. teleconnections in DJF: System 4 (from Nov.)

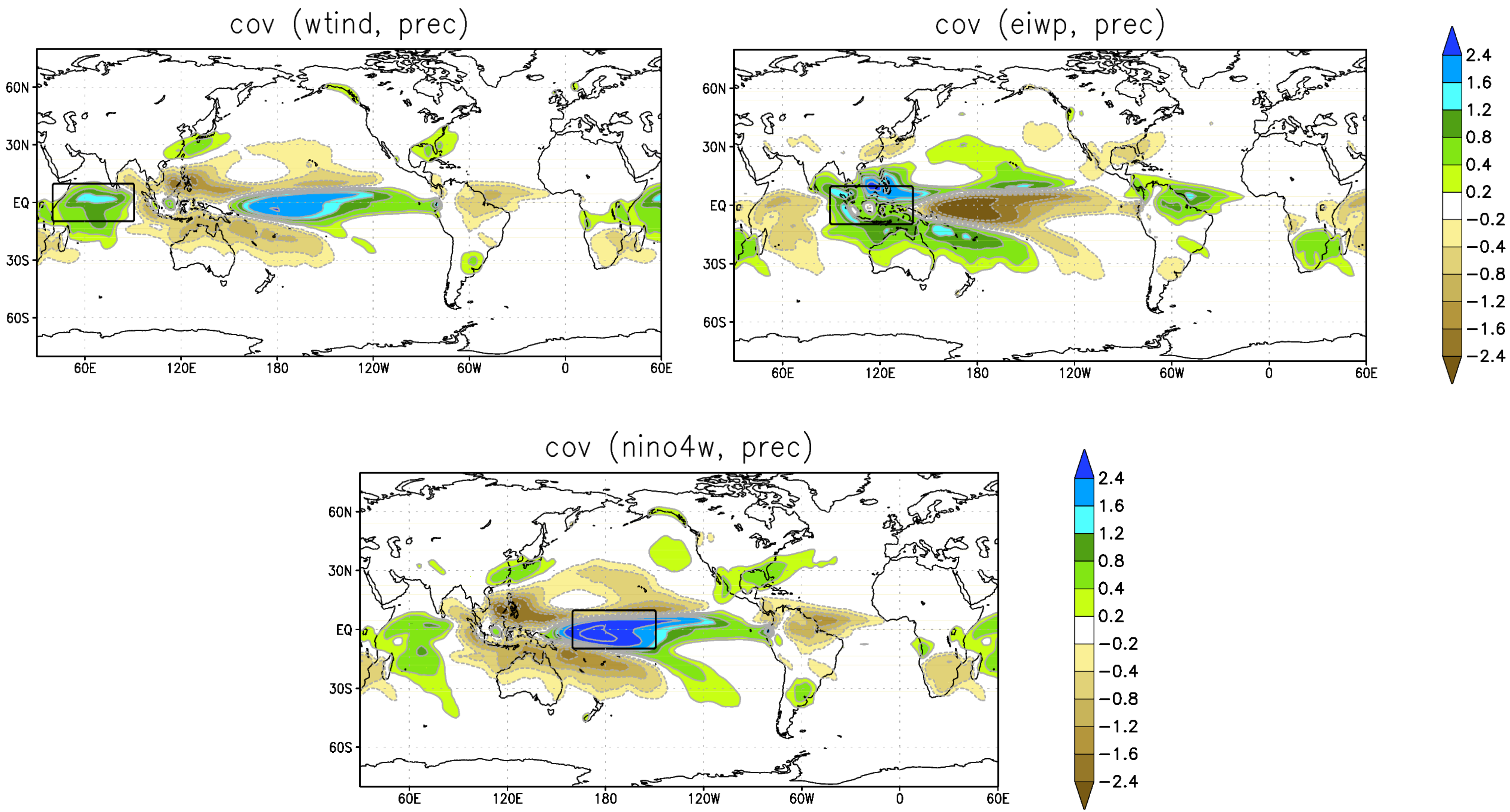

Z 500 hPa vs. SST: ERA-Int. and System-4

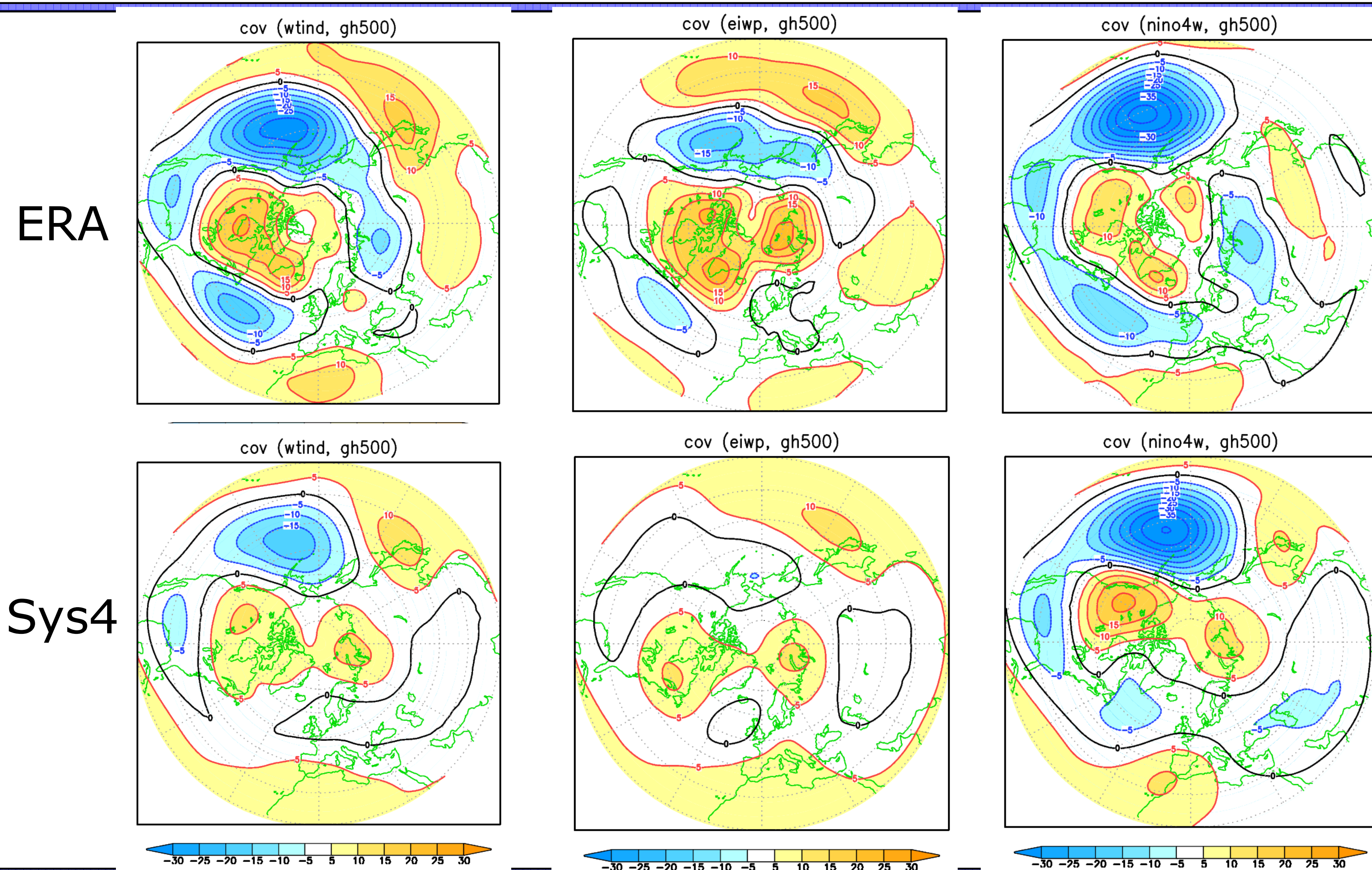

Z 500 hPa vs. precip: ERA-Int. and System-4

ERA

Sys4

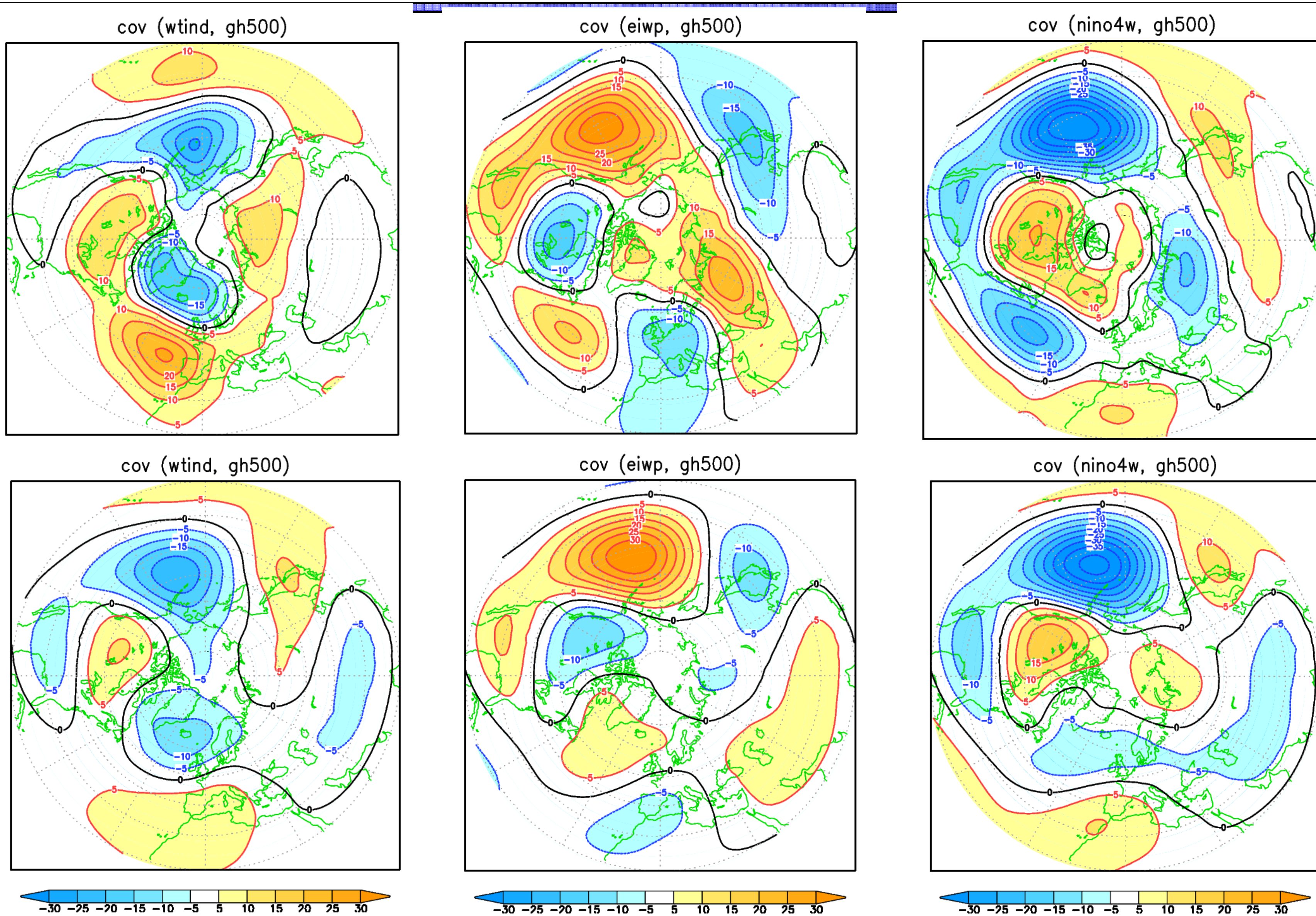

W. Indian Oc. teleconnections, ENSO removed

Full precip anomaly

Anomaly orthogonal to Nino3.4 SST

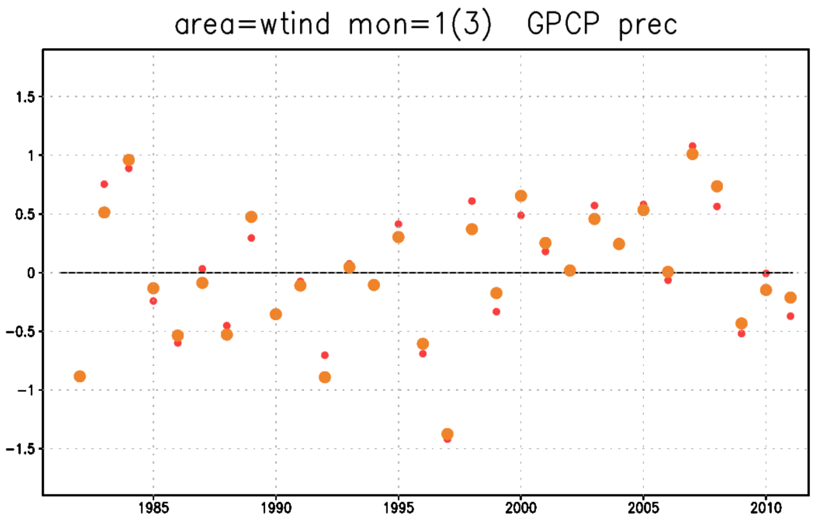

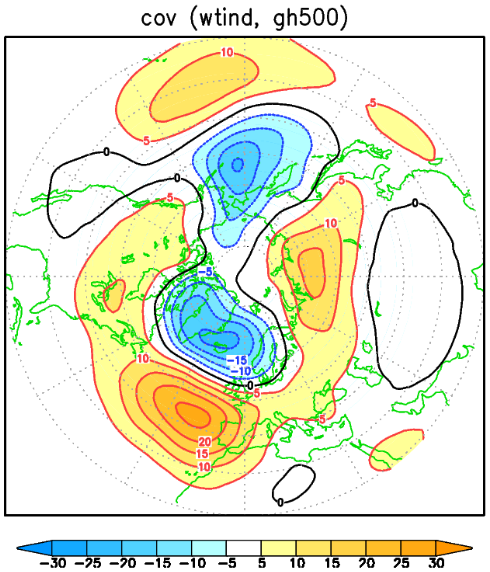

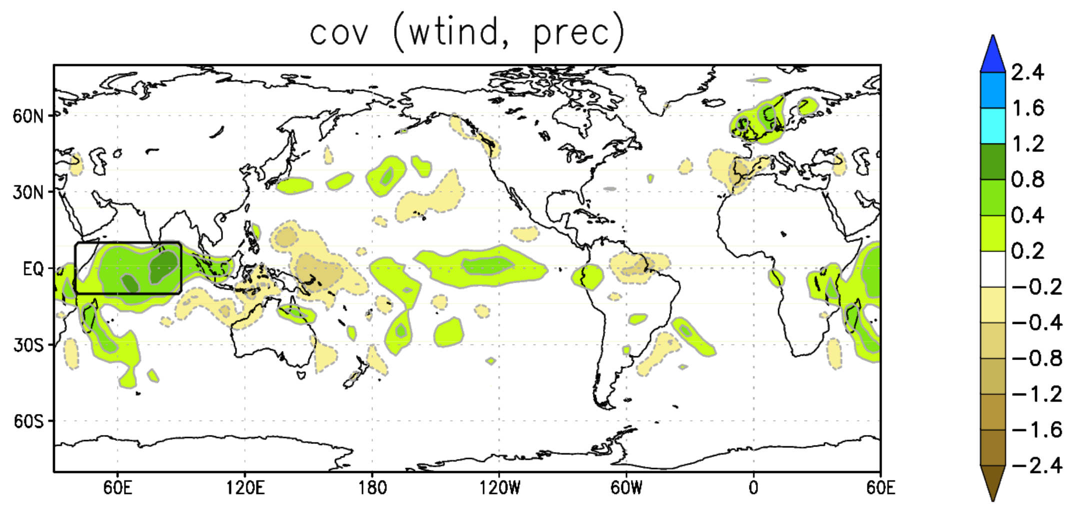

MJO impact on DJF precipitation (Vitart & Molteni 2010)

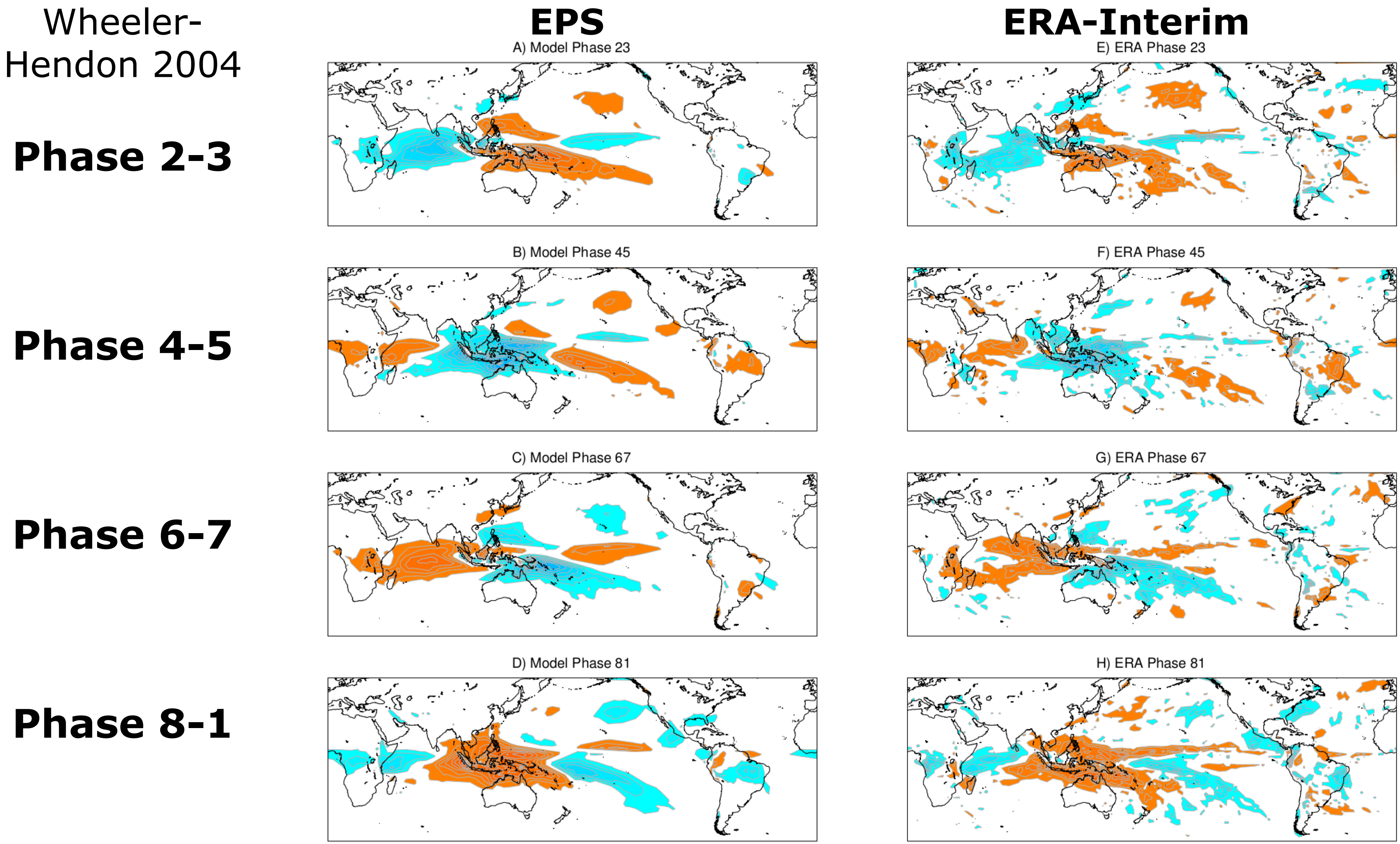

MJO impact on 500-hPa height in DJF (phase 2+3)

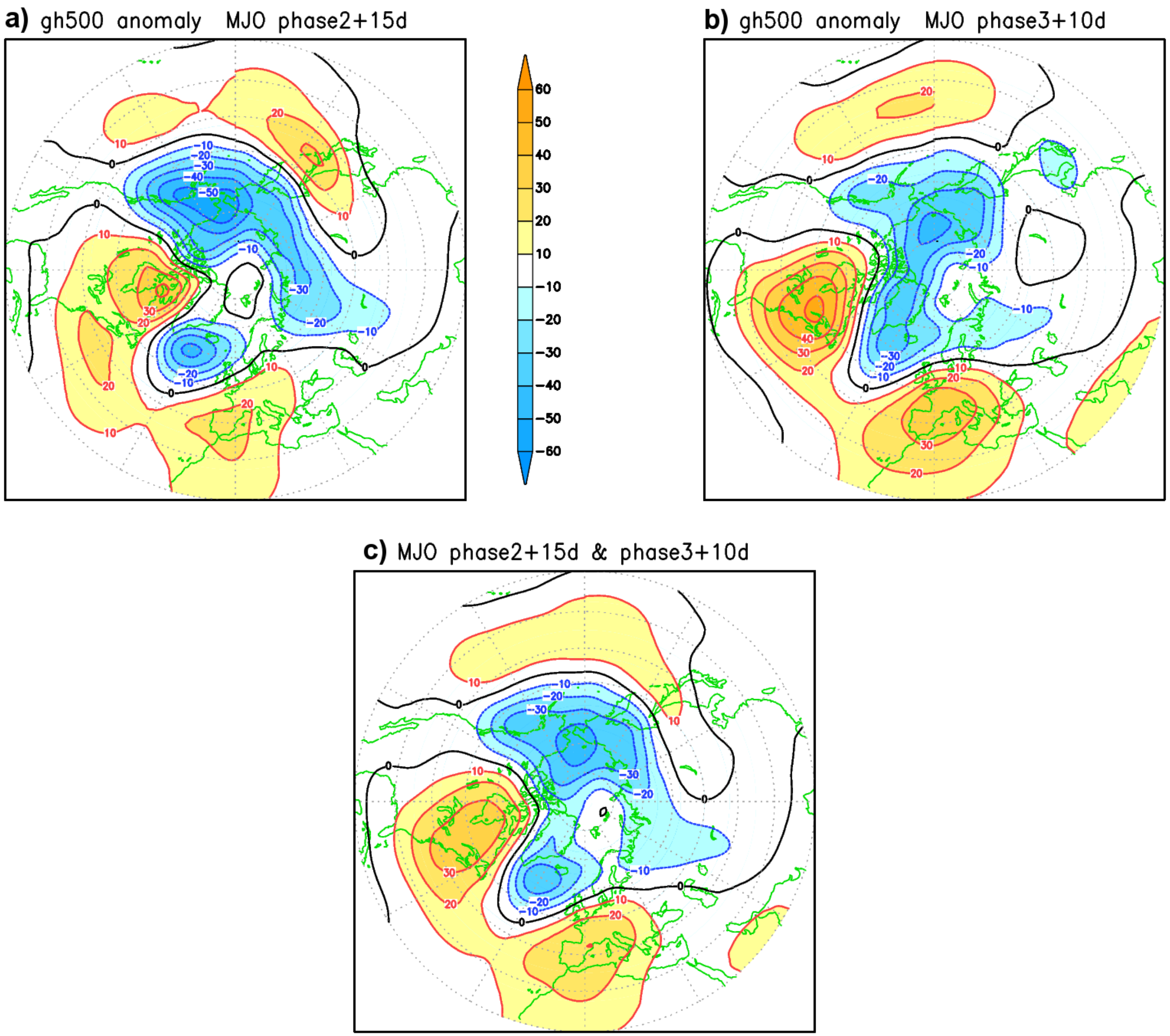

Conclusions

- Teleconnections may be induced either by internal atmospheric dynamics or by coupling with other components of the climate system (mainly the tropical oceans).
- Although a linear interpretation of teleconnection is adequate in most cases, non linear effects should not be neglected.
- Indo-Pacific teleconnections during the northern winter cannot be understood only on the basis of the "SST forces the atmosphere" framework.
- Looking at Indo-Pacific teleconnections in relation to rainfall anomalies (rather than SST) produces more coherent results between observational and model data, and across different time scales (intraseasonal – interannual).
- Periods with increased rainfall over the Western Indian Ocean and reduced rainfall over the eastern Indian – West Pacific Ocean are associated with a positive NAO anomaly in N.H. geopotential height.

References

- Bjerknes, J., 1969: Atmospheric teleconnections from the Equatorial Pacific. Mon. Wea. Rev., **97,** 163–172.
- Gill, A. E., 1980: Some simple solutions for heat-induced tropical circulation. Q. J. R. Meteorol. Soc. **106,** 447-462.
- Horel, J.D. and J.M. Wallace, 1981: Planetary-scale atmospheric phenomena associated with the Southern Oscillation. Mon. Wea. Rev. **109,** 813-829.
- Hoskins, B. J. and D.J. Karoly, 1981: The steady linear response of a spherical atmosphere to thermal and orographic forcing. J. Atmos. Sci. **38,** 1179-1196.
- Molteni, F., T. Stockdale and F. Vitart, 2013: Understanding teleconnections with the Indo-Pacific region during the northern winter. Proceedings of ECMWF Seminar on “Seasonal prediction: science and applications”, pp 47-72.
- Sardeshmukh, P.D. and B.J. Hoskins, 1988: The generation of global rotational flow by steady idealized tropical divergence. J. Atmos. Sci. **45,** 1228–1251.
- Simmons, A. J.; Wallace, J. M.; Branstator, G. W. (1983). Barotropic Wave Propagation and Instability, and Atmospheric Teleconnection Patterns. J. Atmos. Sci. **40,** 1363-1392.
- Van Loon, H. and J.C. Rogers, 1978: The seesaw in winter temperatures between Greenland and Northern Europe. Part I: General description. Mon. Wea. Rev. **106,** 296-310.
- Vitart, F. and F. Molteni, 2010: Simulation of the Madden– Julian Oscillation and its teleconnections in the ECMWF forecast system. Q.J.R. Meteorol. Soc., **136,** 842–855.
- Walker, G.T. and E.W. Bliss, 1932. World Weather V, Memoirs of the Royal Meteorological Society, **4,** (36) , 53-84.
- Wallace, J.M. and D.S. Gutzler, 1981: Teleconnections in the geopotential height field during the Northern Hemisphere winter. Mon. Wea. Rev. **109,** 784-812.
- Wheeler, M.C. and H. H. Hendon, 2004: An all-season real-time multivariate MJO index: Development of an index for monitoring and prediction. Mon. Wea. Rev. **132,** 1917-1932